Theor Chem Acc (2011) 130:115–125
DOI 10.1007/s00214-011-0998-5

REGULAR ARTICLE

Theoretical study on the reactions of trimethylsilane with chlorine and bromine atoms

Yuan Zhang · Hui Zhang · Jing-Yao Liu · Xue-Mei Duan · Ze-Sheng Li

Received: 28 March 2011 / Accepted: 8 July 2011 / Published online: 27 July 2011
© Springer-Verlag 2011

Abstract Theoretical studies are carried out on the multi-channel reactions of $SiH(CH_3)_3$ with Cl (reaction 1, R1) and Br atoms (R2) by direct dynamics method. The minimum energy path is calculated at the MP2/6-31+G(d,p) level, and energetic information is further refined by the MC-QCISD (single-point) method. The rate constants for individual reaction channels, R1a, R1b-in, R1b-out, R1c, R1d, R2a, R2b-in, R2b-out, R2c, and R2d, are calculated by the improved canonical variational transition state theory with small-curvature tunneling correction over the temperature range 200–1,500 K. The theoretical three-parameter expressions $k_1(T) = 6.30 \times 10^{-15} T^{1.36} \exp(704.94/T)$ and $k_2(T) = 9.41 \times 10^{-26} T^{4.89} \exp(-1{,}033.80/T)$ cm^3 $molecule^{-1}$ s^{-1} are given. Our calculations indicate that reaction channels R1c and R2c are the major channel.

Keywords Gas-phase reaction · Transition state · Rate constants

Yuan Zhang and Hui Zhang contributed equally to this work.

Electronic supplementary material The online version of this article (doi:10.1007/s00214-011-0998-5) contains supplementary material, which is available to authorized users.

Y. Zhang
College of Chemistry, Beijing Normal University, Beijing 100875, China

H. Zhang (✉)
College of Chemical and Environmental Engineering, Harbin University of Science and Technology, Harbin 150080, People's Republic of China
e-mail: hust_zhanghui11@hotmail.com

J.-Y. Liu · X.-M. Duan
Institute of Theoretical Chemistry, Jilin University, Changchun 130023, People's Republic of China

Z.-S. Li (✉)
Academy of Fundamental and Interdisciplinary Sciences, Department of Chemistry, Harbin Institute of Technology, Harbin 150080, People's Republic of China
e-mail: zeshengli@hit.edu.cn

Z.-S. Li
School of Sciences, Beijing Institute of Technology, Beijing 100081, People's Republic of China

1 Introduction

Silane and its methyl-substituted homolog are considered as important reagents in plasma chemical vapor deposition (CVD) and in the semiconductor manufacturing process. The use of volatile silicon compounds may lead to their emission into the atmosphere, where they can be removed by reactions with a variety of reactive species, such as hydroxyl, nitrate radicals, and halogen. For most hydrocarbons, hydrogen abstraction by radicals is one of the major channels for their removal in the atmosphere [1, 2]. For the reaction of $SiH(CH_3)_3$ with Cl and Br atoms, the hydrogen atom can be abstracted from SiH group and CH_3 group, Cl or Br atom displacement for hydrogen from SiH group, and CH_3 can be abstracted by Cl or Br atom, as a result, the five reaction pathways are feasible, denoted as follows:

$$\begin{aligned}
Cl + SiH(CH_3)_3 &\rightarrow Si(CH_3)_3 + HCl \quad (R1a)\\
&\rightarrow SiH(CH_3)_2CH_2 + HCl\\
&\quad (R1b\text{-}in \text{ and } R1b\text{-}out)\\
&\rightarrow Si(CH_3)_3Cl + H \quad (R1c)\\
&\rightarrow SiH(CH_3)_2 + CH_3Cl \quad (R1d)\\
Br + SiH(CH_3)_3 &\rightarrow Si(CH_3)_3 + HBr \quad (R2a)\\
&\rightarrow SiH(CH_3)_2CH_2 + HBr\\
&\quad (R2b\text{-}in \text{ and } R2b\text{-}out)\\
&\rightarrow Si(CH_3)_3Br + H \quad (R2c)\\
&\rightarrow SiH(CH_3)_2 + CH_3Br \quad (R2d)
\end{aligned}$$

In 1992, the rate constants have been measured for the reactions of $SiH(CH_3)_3$ with Cl (R1) and Br atoms (R2) of $k_1 = (1.24 \pm 0.35) \times 10^{-10}$ exp(1.3 ± 0.8 kJ mol^{-1}/*RT*) and $k_{2a} = (7.6 \pm 3.3) \times 10^{-10}$exp(−28.4 ± 1.3 kJ mol^{-1}/*RT*) cm^3 molecule^{-1} s^{-1} over the temperature range of 300–460 K by Ding et al. [3]. Because measurements were taken mostly at the lower temperature range of practical interest and no experimental information is available on the branching ratios of the title reaction, theoretical investigation is desirable to give a further understanding of the mechanism of this multi-channel reaction and to evaluate the rate constant at high temperatures. To the best of our knowledge, no previous theoretical work has been performed on this reaction.

In this paper, dual-level direct dynamics method [4–8] is employed to study the kinetics of the title reaction. The potential energy surface (PES) information including geometries, energies, gradients, force constants of all the stationary points (reactants, complexes, products, and transition states) and some extra points along the minimum energy path (MEP) are obtained directly from electronic structure calculations. Single-point energies are calculated by the MC-QCISD method [9]. The calculations indicate that two reaction routes exist in the reaction channels R1b and R2b, respectively, namely "in-plane hydrogen abstraction" (channels R1b-in and R2b-in) and "out-of-plane hydrogen abstraction" (channels R1b-out and R2b-out). Both pathways "in-plane hydrogen abstraction" and "out-of-plane hydrogen abstraction" lead to the same products, and the reaction route of the abstraction from the in-plane hydrogen has a lower barrier than the other route. Subsequently, by means of POLYRATE 9.1 program [10], the rate constants of these reaction channels are calculated by the variational transition state theory (VTST) [11, 12] proposed by Truhlar et al. The comparison between the theoretical and experimental results is discussed. Our results may be helpful for further experimental investigations.

2 Computational method

In the present work, the equilibrium geometries and frequencies of all the stationary points (reactants, complexes, products, and transition states) are optimized at the restricted or unrestricted second-order Møller-Plesset perturbation (MP2) [13–15] level with the 6-31+G(d,p) basis set. The MEP is obtained by intrinsic reaction coordinate (IRC) theory with a gradient step-size of 0.05 (amu)$^{1/2}$ bohr. Then, the first and second energy derivatives are obtained to calculate the curvature of the reaction path and the generalized vibrational frequencies along the reaction path. In order to obtain more accurate energies and barrier heights, the energies are refined by the MC-QCISD method (multi-coefficient correlation method based on quadratic configuration interaction with single and double excitations proposed by Fast and Truhlar) [9] based on the MP2/6-31+G(d,p) geometries. All the electronic structure calculations are performed by GAUSSIAN03 program package [16].

VTST [11, 12] is employed to calculate the rate constants by the POLYRATE 9.1 program [10]. The theoretical rate constants for each reaction channel over the temperature range 200–1,500 K are calculated by the improved canonical variational transition state theory (ICVT) [17] incorporating small-curvature tunneling (SCT) [18, 19] contributions proposed by Truhlar et al. [17]. For the title reaction, most of the vibrational modes are treated as quantum–mechanical separable harmonic oscillators except for the lowest modes. The hindered-rotor approximation of Truhlar and Chuang [20, 21] is used for calculating the partition function of the ten transition state modes. The curvature components are calculated by using a quadratic fit to obtain the derivative of the gradient with respect to the reaction coordinate. Since $SiH(CH_3)_3$ is C_{3V} symmetry, there are "in-plane hydrogen abstraction" and "out-of-plane hydrogen abstraction" for the reaction channels R1b and R2b; the symmetry factor $\sigma = 3, 6$ for the "in-plane hydrogen abstraction" and "out-of-plane hydrogen abstraction" is taken into account in the rate constant calculation, respectively. The total rate constants are calculated from the sum of the individual rate constants, i.e., $k_n = k_{na} + k_{nb} + k_{nc} + k_{nd}$, where $k_{nb} = k_{nb\text{-}in} + k_{nb\text{-}out}$ ($n = 1, 2$).

3 Results and discussions

3.1 Stationary points

The optimized geometries of the reactant ($SiH(CH_3)_3$), complexes (CR1aR, CR1aF, CR1bR-in, CR1bR-out,

CR1bF-out, CR1cR, CR2bF-in, and CR2bF-out), products ($Si(CH_3)_3$, $SiH(CH_3)_2CH_2$, HCl, $Si(CH_3)_3Cl$, $SiH(CH_3)_2$, CH_3Cl, HBr, $Si(CH_3)_3Br$, and CH_3Br), and transition states (TS1a, TS1b-in, TS1b-out, TS1c, TS1d, TS2a, TS2b-in, TS2b-out, TS2c, and TS2d) calculated at the MP2/6-31+G(d,p) level are presented in Fig. 1, along with the available experimental values [22, 23]. The theoretical geometric parameters of HCl, HBr, CH_3Cl, and CH_3Br are in good agreement with the corresponding experimental values [22, 23]. Furthermore, the complexes (CR1aR, CR1bR-in, CR1bR-out, and CR1cR) are located on the reactant sides for the reaction R1. At the MP2 level, the distances between the hydrogen atom in SiH or CH_3 group of $SiH(CH_3)_3$ and the chlorine atom in CR1aR, CR1bR-in, CR1bR-out, and CR1cR are 3.720, 3.463, 3.353, and 3.284 Å in CR1aR, CR1bR-in, CR1bR-out, and CR1cR, respectively, while the other bond lengths are very close to those of the reactant. On the product sides of reaction R1a,

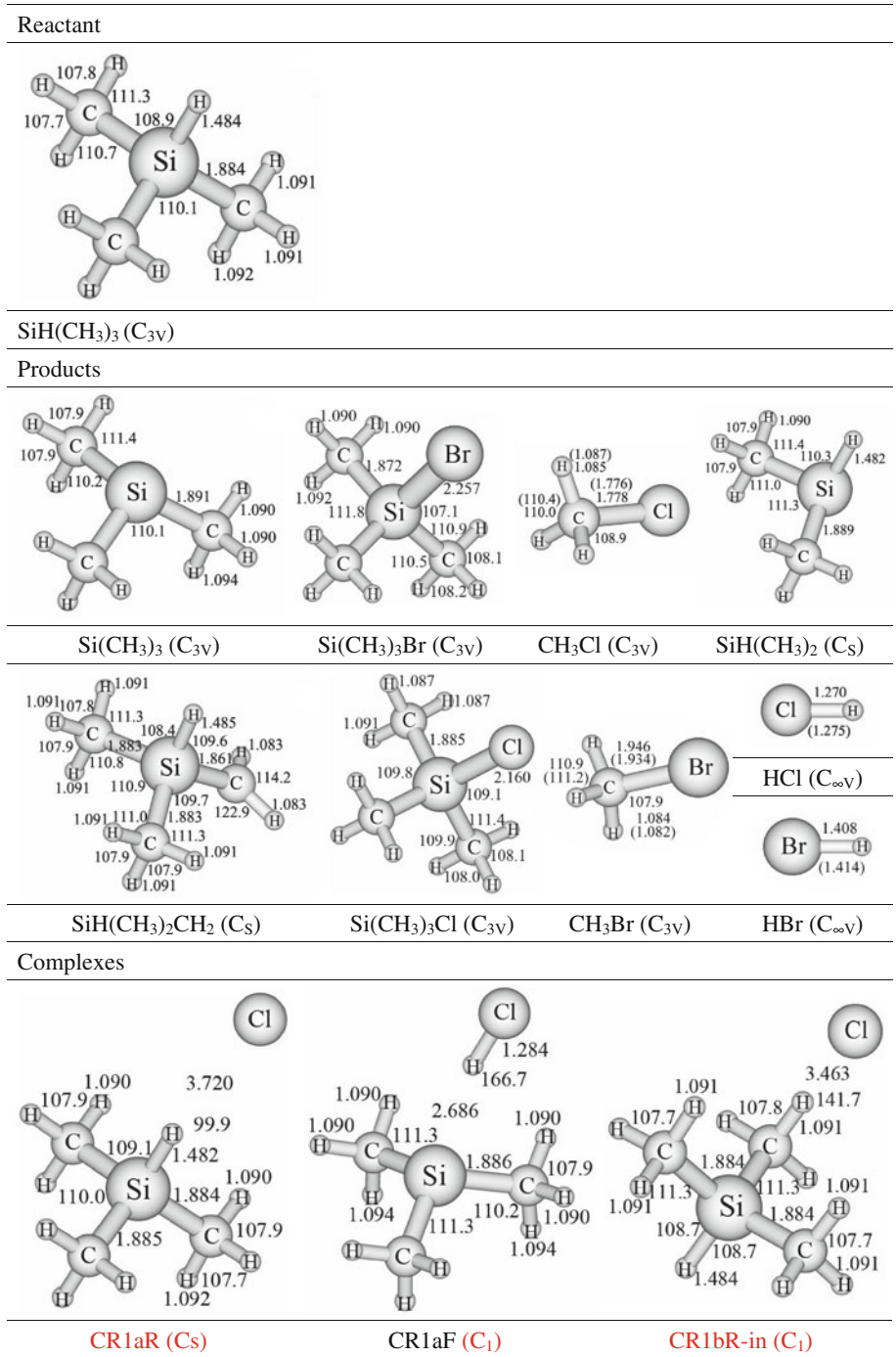

Fig. 1 Optimized geometries of the reactants, complexes, products, and transition states at the MP2/6-31+G(d,p) level. The values in *parentheses* are the experimental values (Ref. [22] for CH_3Cl and CH_3Br, and Ref. [23] for HCl and HBr). Bond lengths are in angstrom, and angles are in degree

Fig. 1 continued

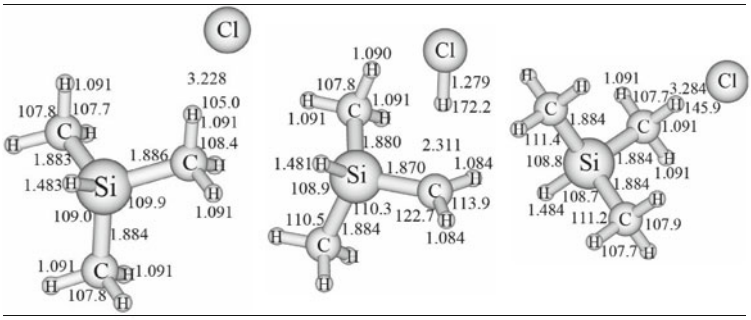

CR1bR-out (Cs) CR1bF-out (C_1) CR1cR (C_1)

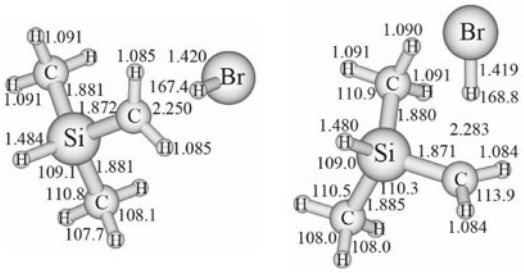

CR2bF-in (C_1) CR2bF-out (C_1)

Transition States

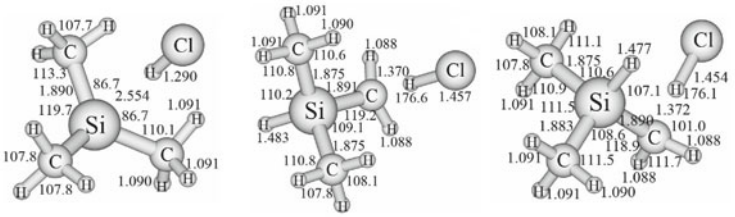

TS1a (C_{3V}) TS1b-in (C_1) TS1b-out (C_1)

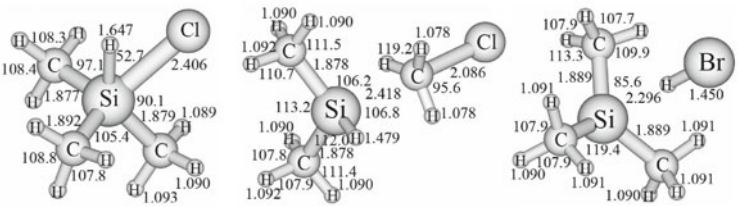

TS1c (C_1) TS1d (C_1) TS2a (C_{3V})

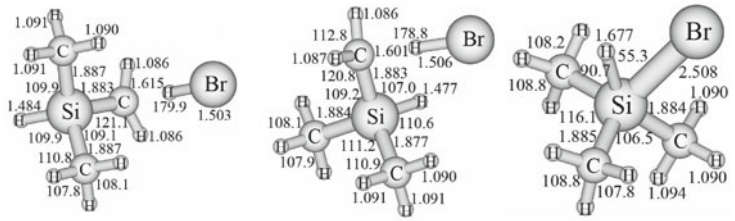

TS2b-in (C_1) TS2b-out (C_1) TS2c (C_1)

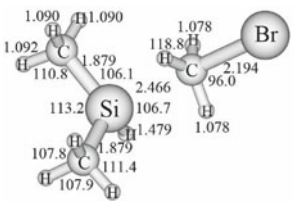

TS2d (C_1)

R1b-out, R2b-in, and R2b-out, there are four hydrogen-bonded complexes (CR1aF, CR1bF-out, CR2bF-in, and CR2bF-out); the distance between the silicon or carbon atom in SiH or CH_3 group of $Si(CH_3)_4$ and the hydrogen atom of the HCl or HBr in CR1aF, CR1bF-out, CR2bF-in, and CR2bF-out are 2.686, 2.311, 2.250, and 2.283 Å, respectively, while the other bond lengths are very close to those of the products. Figure 1 shows that the transition states TS1b, TS1c, TS1d, TS2b, TS2c, and TS2d have the same symmetry, C_1, when symmetries of TS1b-in and TS2b-in are restricted to C_S, the corresponding frequencies have three and four imaginary frequencies at the same level, respectively, and the transition state TS1a and TS2a have C_{3V} symmetry. In TS2a, TS2b-in, and TS2b-out structures, the breaking bonds Si–H, C–H, and C–H increase by 55, 48, and 47% compared with the equilibrium bond length in $SiH(CH_3)_3$, respectively; the forming bonds H–Br stretch by 3, 7, and 7% over the equilibrium bond lengths in isolated HBr, respectively. The elongation of the breaking bond is larger than that of the forming bond, indicating that TS2a, TS2b-in, and TS2b-out of the title reaction systems are all product-like, i.e., the three reaction channels will proceed via "late" transition states, which is consistent with Hammond's postulate [24], applied to for an endothermic reaction.

Table 1 lists the harmonic vibrational frequencies of the reactants, complexes, products, and transition states calculated at the MP2/6-31+G(d,p) level as well as the available experimental values [25–27]. For the species CH_3Cl, CH_3Br, HCl, and HBr, the calculated frequencies are in good agreement with the experimental values with the largest deviation of 7%. The ten transition states are all confirmed by normal-mode analysis to have one and only one imaginary frequency, which corresponds to the stretching modes of coupling between breaking and forming bonds. And the values of those imaginary frequencies are $422i$ cm^{-1} for TS1a, $1{,}157i$ cm^{-1} for TS1b-in, $1{,}182i$ cm^{-1} for TS1b-out, $326i$ cm^{-1} for TS1c, and $753i$ cm^{-1} for TS1d, $438i$ cm^{-1} for TS2a, $349i$ cm^{-1} for TS2b-in, $381i$ cm^{-1} for TS2b-out, $277i$ cm^{-1} for TS2c, and $694i$ cm^{-1} for TS2d.

3.2 Energetics

The reaction enthalpies (ΔH^0_{298}) and potential barrier heights (ΔE^{TS}) with zero-point energy (ZPE) corrections for the title reactions of $SiH(CH_3)_3$ with Cl and Br atoms calculated at the MC-QCISD//MP2/6-31+G(d,p) level are listed in Table 2. The values calculated agree well with the corresponding experimental value. The theoretical values at 298 K of ΔH^0_{298}, –10.9 and 2.8 kcal/mol for the reactions R1a and R2a, are in good agreement with the corresponding experimental values –8.0 ± 2.6 and 5.4 ± 2.6 kcal/mol, respectively, which were derived from the standard heats of formation (Cl, 28.97 kcal/mol [27]; Br, 26.72 kcal/mol [27]; $SiH(CH_3)_3$, −39.00 ± 0.96 kcal/mol [28]; $Si(CH_3)_3$, 4.07 ± 1.67 kcal/mol [3]; HCl, −22.05 kcal/mol [27]; HBr, −8.70 kcal/mol [27]). So the values calculated at MC-QCISD//MP2/6-31+G(d,p) level are expected to be reliable. Thus, in the present study, we use MC-QCISD//MP2/6-31+G(d,p) method to calculate the potential energy barriers as well as the energies along the MEP in the following studies.

The schematic potential energy surfaces of the $SiH(CH_3)_3$ with Cl and Br atoms reaction with ZPE corrections obtained at the MC-QCISD//MP2/6-31+G(d,p) level are plotted in Figs. 2 and 3. Note that the energy of reactant is set to zero for reference. The values in parentheses are calculated at the MP2/6-31+G(d,p) level and include the ZPE corrections. For reaction R1, the attack of Cl atom on Si–H or C–H bond would proceed via the reactant complexes (CR1aR, CR1bR-in, CR1bR-out, and CR1cR), which are about 2.87, 3.69, 3.87, 5.00 kcal/mol lower than that of the corresponding reactants at the MC-QCISD level. For reaction R1a, R1b, and R2b, the complex (CR1aF, CR1bF-out, CR2bF-in, and CR2bF-out) with the energy of 3.70, 2.14, 2.18, and 1.87 kcal/mol lower than that of the products is located at the product side at the MC-QCISD/MP2/6-31+G(d,p) level involving ZPE correction. The potential barrier heights of the reaction channel R1c (−4.13 kcal/mol) are much lower than those of R1b-in (−3.02 kcal/mol), R1b-out (−2.24 kcal/mol), and R1d (22.72 kcal/mol) at MC-QCISD//MP2/6-31+G(d,p) level. At the same time, the former reaction path R1c is more exothermic than the later by about 15.43, 22.90, and 35.15 kcal/mol for R1a, R1b-in (or R1b-out), and R1d, respectively, and as a result, the former reaction path R1c is more thermodynamically and kinetically favorable than the later. Thus, we infer that the reaction channel R1c is the dominant channel for the reaction of $SiH(CH_3)_3$ with Cl atom. A similar order of energies can be obtained from the reaction of $SiH(CH_3)_3$ with Br atom. We use the formula $E_{a,298} = \Delta E^* + RT = V^* + \Delta ZPE + \Delta E\ (T) + RT$ as a simple estimation of the activation energy [29], where V^* and $\Delta E\ (T)$ represent the potential barrier height and thermal energy correction; the estimated activation energies are −1.52, −7.20, −6.40, and −5.32 kcal/mol for the four reaction channels R1a, R1b-in, R1b-out, and R1c, respectively, which means that the four reaction channels are barrierless. The negative activation energy results in the negative temperature dependence. We perform the rate constant calculations for the ten channels of reaction of $SiH(CH_3)_3$ with Cl and Br in the following work.

Table 1 Calculated and experimental frequencies (in cm^{-1}) for the reactants, complexes, products, and transition states for the title reaction at the MP2/6-31+G(d,p) level

Species	MP2/6-31+G(d,p)	Expt.
$SiH(CH_3)_3$	3,215, 3,215, 3,215, 3,210, 3,209, 3,209, 3,111, 3,111, 3,111, 2,280, 1,513, 1,504, 1,504, 1,495, 1,495, 1,490, 1,350, 1,340, 1,340, 952, 952, 908, 882, 882, 729, 729, 706, 637, 637, 633, 239, 200, 200, 169, 169, 142	
$Si(CH_3)_3$	3,222, 3,222, 3,222, 3,197, 3,197, 3,197, 3,101, 3,101, 3,100, 1,508, 1,498, 1,498, 1,491, 1,491, 1,485, 1,342, 1,330, 1,330, 902, 897, 897, 749, 749, 715, 706, 706, 618, 227, 197, 197, 156, 156, 132	
$SiH(CH_3)_2CH_2$	3,327, 3,225, 3,216, 3,216, 3,215, 3,214, 3,113, 3,113, 2,267, 1,508, 1,503, 1,497, 1,495, 1,472, 1,346, 1,339, 948, 945, 893, 863, 764, 755, 728, 697, 645, 635, 564, 252, 210, 199, 173, 158, 91	
HCl	3,112	2,991[a]
$Si(CH_3)_3Cl$	3,223, 3,223, 3,222, 3,212, 3,211, 3,211, 3,112, 3,112, 3,112, 1,511, 1,499, 1,499, 1,491, 1,491, 1,485, 1,352, 1,342, 1,342, 906, 904, 904, 802, 802, 721, 721, 716, 654, 499, 231, 231, 220, 181, 181, 175, 175, 154	
$SiH(CH_3)_2$	3,227, 3,227, 3,207, 3,207, 3,111, 3,110, 2,282, 1,501, 1,498, 1,493, 1,489, 1,343, 1,335, 934, 908, 896, 758, 714, 661, 630, 529, 201, 156, 132	
CH_3Cl	3,278, 3,278, 3,161, 1,525, 1,525, 1,458, 1,074, 1,074, 781	3,039[b], 2,937, 1,452, 1,355, 1,017, 732
HBr	2,733	2,649[c]
$Si(CH_3)_3Br$	3,226, 3,226, 3,225, 3,211, 3,210, 3,210, 3,111, 3,111, 3,111, 1,509, 1,501, 1,501, 1,491, 1,491, 1,488, 1,350, 1,340, 1,340, 906, 906, 902, 801, 801, 723, 723, 720, 644, 399, 218, 218, 197, 194, 194, 170, 160, 160	
CH_3Br	3,291, 3,291, 3,164, 1,525, 1,525, 1,399, 1,009, 1,009, 632	3,056[b], 2,972, 1,443, 1,306, 955, 611
CR1aR	3,218, 3,217, 3,214, 3,210, 3,209, 3,209, 3,112, 3,111, 3,110, 2,285, 1,513, 1,503, 1,502, 1,496, 1,496, 1,487, 1,348, 1,338, 1,335, 951, 944, 908, 882, 881, 728, 726, 706, 638, 636, 633, 239, 201, 200, 169, 165, 140, 36, 33, 26	
CR1bR-in	3,234, 3,215, 3,214, 3,214, 3,213, 3,212, 3,113, 3,112, 3,112, 2,278, 1,716, 1,512, 1,500, 1,497, 1,493, 1,491, 1,347, 1,338, 1,335, 1,001, 945, 908, 887, 879, 734, 727, 707, 637, 635, 632, 238, 229, 200, 195, 167, 141, 35, 32, 18	
CR1bR-out	3,215, 3,215, 3,211, 3,211, 3,210, 3,204, 3,111, 3,111, 3,107, 2,281, 1,512, 1,505, 1,502, 1,495, 1,494, 1,490, 1,348, 1,340, 1,333, 951, 950, 908, 882, 879, 729, 727, 706, 637, 636, 633, 239, 202, 201, 182, 174, 150, 38, 33, 20	
CR1cR	3,223, 3,222, 3,212, 3,211, 3,210, 3,113, 3,112, 3,112, 1,511, 1,499, 1,499, 1,491, 1,491, 1,486, 1,352, 1,342, 1,342, 906, 904, 904, 802, 801, 721, 721, 716, 654, 499, 231, 231, 220, 181, 181, 176, 175, 154, 59, 29, 23	
CR1aF	3,225, 3,225, 3,224, 3,200, 3,200, 3,199, 3,103, 3,103, 3,102, 2,880, 1,507, 1,497, 1,496, 1,490, 1,489, 1,484, 1,345, 1,333, 1,332, 901, 901, 900, 754, 754, 719, 710, 710, 618, 353, 348, 228, 197, 197, 160, 153, 133, 58, 25, 13	
CR1bF-out	3,317, 3,223, 3,220, 3,215, 3,214, 3,212, 3,115, 3,113, 2,977, 2,294, 1,508, 1,501, 1,496, 1,493, 1,470, 1,349, 1,338, 946, 943, 900, 869, 792, 750, 727, 665, 645, 635, 603, 308, 266, 244, 217, 206, 175, 155, 116, 80, 41, 29	
CR2aF-in	3,315, 3,224, 3,224, 3,215, 3,214, 3,212, 3,116, 3,115, 2,552, 2,272, 1,510, 1,505, 1,500, 1,495, 1,468, 1,350, 1,343, 950, 943, 899, 866, 771, 749, 732, 697, 644, 639, 595, 330, 310, 258, 213, 202, 181, 169, 146, 80, 60, 59	
CR2bF-out	3,317, 3,227, 3,220, 3,215, 3,214, 3,211, 3,115, 3,113, 2,577, 2,297, 1,511, 1,501, 1,496, 1,493, 1,469, 1,348, 1,338, 945, 944, 901, 870, 794, 749, 726, 666, 645, 637, 605, 315, 293, 245, 219, 208, 180, 163, 121, 70, 56, 36	
TS1a	3,213, 3,213, 3,212, 3,208, 3,208, 3,206, 3,112, 3,112, 3,111, 2,774, 1,517, 1,517, 1,504, 1,486, 1,483, 1,483, 1,356, 1,342, 1,342, 901, 901, 834, 834, 753, 746, 746, 728, 579, 361, 361, 200, 200, 70, 62, 54, 54, 16, 16, 422*i*	
TS1b-in	3,279, 3,223, 3,223, 3,217, 3,217, 3,182, 3,117, 3,116, 2,278, 1,506, 1,502, 1,495, 1,492, 1,456, 1,351, 1,345, 1,102, 979, 950, 933, 899, 866, 844, 738, 732, 704, 675, 640, 639, 479, 417, 256, 203, 201, 163, 147, 83, 53, 1,157*i*	
TS1b-out	3,278, 3,227, 3,222, 3,214, 3,213, 3,181, 3,116, 3,114, 2,317, 1,507, 1,500, 1,494, 1,492, 1,456, 1,349, 1,339, 1,100, 978, 944, 937, 905, 871, 840, 755, 727, 720, 656, 639, 639, 476, 414, 236, 208, 184, 168, 150, 78, 48, 1,182*i*	

Table 1 continued

Species	MP2/6-31+G(d,p)	Expt.
TS1c	3,233, 3,228, 3,226, 3,211, 3,210, 3,205, 3,112, 3,109, 3,106, 1,510, 1,500, 1,496, 1,492, 1,490, 1,483, 1,350, 1,343, 1,330, 1,320, 918, 908, 902, 856, 812, 788, 732, 723, 701, 617, 506, 258, 242, 221, 211, 182, 171, 142, 26, 326*i*	
TS1d	3,386, 3,382, 3,226, 3,226, 3,209, 3,208, 3,189, 3,112, 3,112, 2,303, 1,500, 1,496, 1,490, 1,487, 1,436, 1,434, 1,349, 1,341, 1,064, 1,055, 1,027, 932, 903, 889, 778, 723, 668, 635, 577, 261, 234, 232, 184, 154, 142, 95, 77, 54, 753*i*	
TS2a	3,212, 3,212, 3,212, 3,211, 3,211, 3,209, 3,111, 3,111, 3,111, 2,091, 1,516, 1,516, 1,502, 1,485, 1,482, 1,482, 1,355, 1,342, 1,342, 901, 901, 835, 835, 754, 747, 747, 728, 578, 422, 422, 204, 204, 76, 70, 70, 69, 41, 41, 438*i*	
TS2b-in	3,297, 3,224, 3,224, 3,216, 3,216, 3,196, 3,116, 3,116, 2,276, 1,508, 1,502, 1,497, 1,493, 1,462, 1,359, 1,344, 1,344, 950, 938, 900, 872, 779, 740, 737, 708, 696, 675, 641, 639, 573, 361, 255, 206, 200, 170, 152, 71, 59, 349*i*	
TS2b-out	3,297, 3,228, 3,222, 3,214, 3,213, 3,196, 3,115, 3,114, 2,314, 1,509, 1,500, 1,495, 1,492, 1,462, 1,348, 1,338, 1,305, 943, 935, 904, 874, 800, 746, 728, 718, 698, 660, 641, 634, 562, 358, 239, 207, 189, 172, 155, 68, 45, 381*i*	
TS2c	3,233, 3,227, 3,226, 3,209, 3,208, 3,205, 3,109, 3,109, 3,104, 1,508, 1,502, 1,497, 1,492, 1,490, 1,484, 1,343, 1,332, 1,327, 1,207, 912, 902, 896, 826, 809, 740, 737, 726, 691, 614, 528, 254, 246, 215, 214, 177, 152, 148, 46, 277*i*	
TS2d	3,388, 3,385, 3,226, 3,225, 3,208, 3,208, 3,194, 3,112, 3,111, 2,302, 1,500, 1,495, 1,490, 1,486, 1,444, 1,444, 1,348, 1,340, 1,041, 1,039, 997, 932, 902, 887, 776, 722, 667, 635, 567, 255, 229, 219, 176, 147, 134, 82, 73, 51, 694*i*	

[a] Ref. [25]

[b] Ref. [26]

[c] Ref. [27]

Table 2 The reaction enthalpies at 298 K (ΔH^0_{298}), the barrier heights TSs (ΔE^{TS}) (kcal/mol) with zero-point energy (ZPE) correction for the reactions of Cl and Br atoms with $SiH(CH_3)_3$ at the MC-QCISD//MP2/6-31+G(d,p) level together with the experimental value

		MC-QCISD//MP2	Expt.
ΔH^0_{298}	$Cl + SiH(CH_3)_3 \rightarrow Si(CH_3)_3 + HCl$ (R1a)	−10.89	−7.95 ± 2.63
	$Cl + SiH(CH_3)_3 \rightarrow SiH(CH_3)_2CH_2 + HCl$ (R1b-in)	−3.30	
	$Cl + SiH(CH_3)_3 \rightarrow SiH(CH_3)_2CH_2 + HCl$ (R1b-out)	−3.30	
	$Cl + SiH(CH_3)_3 \rightarrow SiH(CH_3)_2Cl + H$ (R1c)	−26.20	
	$Cl + SiH(CH_3)_3 \rightarrow SiH(CH_3)_2 + CH_3Cl$ (R1d)	8.12	
	$Br + SiH(CH_3)_3 \rightarrow Si(CH_3)_3 + HBr$ (R2a)	2.84	5.40 ± 2.63
	$Br + SiH(CH_3)_3 \rightarrow SiH(CH_3)_2CH_2 + HBr$ (R2b-in)	10.43	
	$Br + SiH(CH_3)_3 \rightarrow SiH(CH_3)_2CH_2 + HBr$ (R2b-out)	10.43	
	$Br + SiH(CH_3)_3 \rightarrow SiH(CH_3)_2Br + H$ (R2c)	−10.66	
	$Br + SiH(CH_3)_3 \rightarrow SiH(CH_3)_2 + CH_3Br$ (R2d)	18.70	
ΔE^{TS} + ZPE	$Cl + SiH(CH_3)_3 \rightarrow Si(CH_3)_3 + HCl$ (R1a)	−1.40	
	$Cl + SiH(CH_3)_3 \rightarrow SiH(CH_3)_2CH_2 + HCl$ (R1b-in)	−3.02	
	$Cl + SiH(CH_3)_3 \rightarrow SiH(CH_3)_2CH_2 + HCl$ (R1b-out)	−2.24	
	$Cl + SiH(CH_3)_3 \rightarrow SiH(CH_3)_2Cl + H$ (R1c)	−4.13	
	$Cl + SiH(CH_3)_3 \rightarrow SiH(CH_3)_2 + CH_3Cl$ (R1d)	22.72	
	$Br + SiH(CH_3)_3 \rightarrow Si(CH_3)_3 + HBr$ (R2a)	11.14	
	$Br + SiH(CH_3)_3 \rightarrow SiH(CH_3)_2CH_2 + HBr$ (R2b-in)	7.44	
	$Br + SiH(CH_3)_3 \rightarrow SiH(CH_3)_2CH_2 + HBr$ (R2b-out)	8.02	
	$Br + SiH(CH_3)_3 \rightarrow SiH(CH_3)_2Br + H$ (R2c)	4.93	
	$Br + SiH(CH_3)_3 \rightarrow SiH(CH_3)_2 + CH_3Br$ (R2d)	29.67	

Experimental value derived from the standard heats of formation (in kcal/mol): Cl, 28.97 kcal/mol [27]; Br, 26.72 kcal/mol [27]; $SiH(CH_3)_3$, −39.00 ± 0.96 kcal/mol [28]; $Si(CH_3)_3$, 4.07 ± 1.67 kcal/mol [3]; HCl, −22.05 kcal/mol [27]; HBr, −8.70 kcal/mol [27]

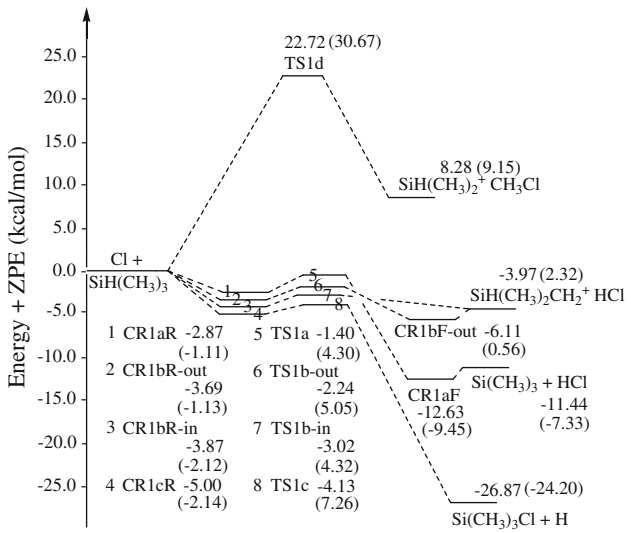

Fig. 2 Schematic potential energy surface for Cl + $SiH(CH_3)_3$ reaction system. Relative energies are calculated at the MC-QCISD//MP2/6-31+G(d,p) + ZPE level. The values in *parentheses* are calculated at the MP2/6-31+G(d,p) + ZPE level [in (kcal/mol)]

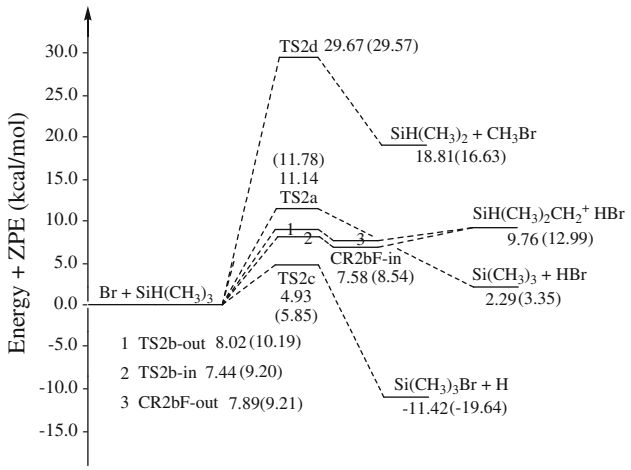

Fig. 3 Schematic potential energy surface for Br + $SiH(CH_3)_3$ reaction system. Relative energies are calculated at the MC-QCISD//MP2/6-31+G(d,p) + ZPE level. The values in *parentheses* are calculated at the MP2/6-31+G(d,p) + ZPE level [in (kcal/mol)]

3.3 Rate constants

Dual-level dynamics calculations [4–8] of the title reaction are carried out at the MC-QCISD//MP2/6-31+G(d,p) level. The rate constants of the individual channel, k_{na}, $k_{nb\text{-}in}$, $k_{nb\text{-}out}$, k_{nc}, and k_{nd} ($n = 1, 2$), are evaluated by conventional transition state theory (TST), the improved canonical variational transition state theory (ICVT), and the ICVT with the small-curvature tunneling (SCT) contributions in a wide temperature range from 200 to 1,500 K. The TST, ICVT, ICVT/SCT rate constants of the ten individual reaction channels, and ICVT/SCT rate constants of k_1 and k_2 are

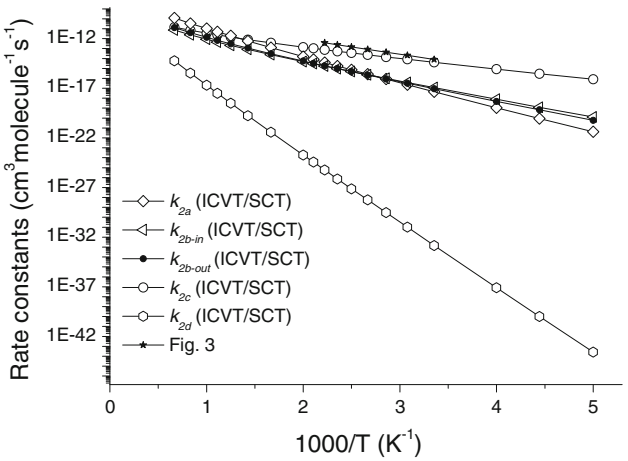

Fig. 4 The ICVT/SCT rate constants calculated at the MC-QCISD//MP2/6-31+G(d,p) level for the five reaction channels of Br + $SiH(CH_3)_3$ (in cm^3 $molecule^{-1}$ s^{-1}) versus 1,000/T between 200 and 1,500 K along with the corresponding experimental results

given in Table S1–4 as supplementary information along with the available experimental results [3]. The calculated rate constant values of k_1 and k_2 at 298 K, 1.56×10^{-10} and 4.10×10^{-15} cm^3 $molecule^{-1}$ s^{-1}, are in good agreement with the available experimental value [3], 2.09×10^{-10} and 7.89×10^{-15} cm^3 $molecule^{-1}$ s^{-1}, and the ratios of $k_{ICVT/SCT}/k$exptl are 0.75 and 0.52 at 298 K. Thus, the present calculation can provide reliable estimations of the rate constants for the title reactions at the higher temperatures.

The calculated ICVT/SCT rate constants of the five reaction channels for reaction R2 are plotted against the reciprocal of temperature in Fig. 4. In Fig. 4, it is shown that the ICVT and TST rate constants of four reaction channels are nearly the same in the whole temperature region, which indicates that the variational effect is almost negligible. And the tunneling effect for the reaction channels R2a and R2d, i.e., the ratio between ICVT/SCT and ICVT rate constants, plays an important role at the lower temperatures and is negligible at high temperatures. For example, the ratios of k(ICVT/SCT)/k(ICVT) are 5.84 and 4.03 at 200 K for R2a and R2d, respectively, and while they are 1.22 and 1.16 at 600 K, respectively. The H-abstraction reaction channels correspond to a heavy-light-heavy mass combination for the R1a, R1b, R2a, and R2b reaction dynamics. When the reaction path is acutely curved as in the H-transfer between two heavy fragments, the SCT method may provide an inadequate account for the tunneling, and the large curvature tunneling (LCT) correction should be more accurate. However, LCT can only be used where an analytic representation of the potential energy surface is available for a reaction, and the large curvature tunneling effect cannot be directly calculated by means of the ab initio PES alone, which is beyond the capabilities of our computational resources. In addition,

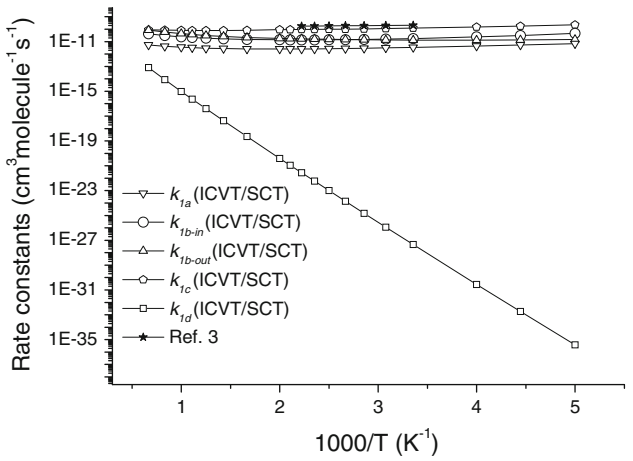

Fig. 5 The ICVT/SCT rate constants calculated at the MC-QCISD//MP2/6-31+G(d,p) level for the five reaction channels of Cl + $SiH(CH_3)_3$ (in cm^3 molecule^{-1} s^{-1}) versus 1,000/T between 200 and 1,500 K along with the corresponding experimental results

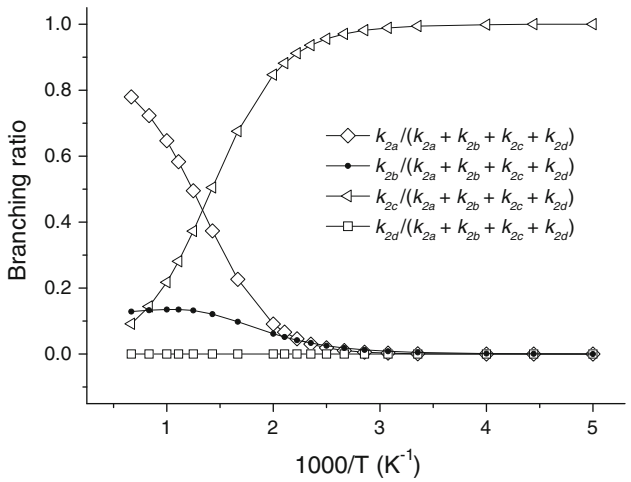

Fig. 6 Calculated branching ratios for the reaction Br + $SiH(CH_3)_3$ versus 1,000/T between 200 and 1,500 K

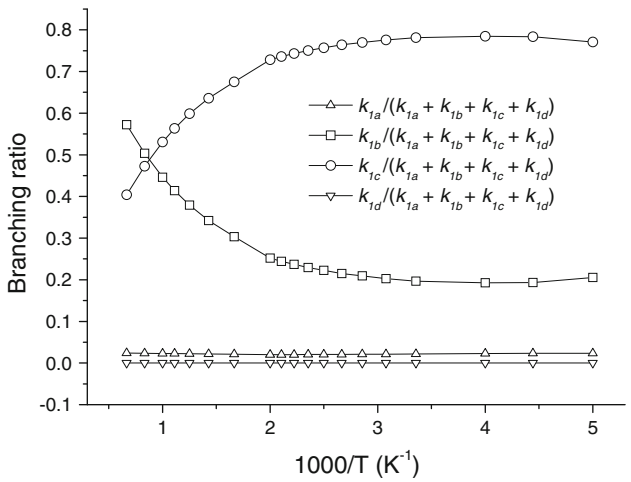

Fig. 7 Calculated branching ratios for the reaction Cl + $SiH(CH_3)_3$ versus 1,000/T between 200 and 1,500 K

our calculated rate constants for the title reactions with SCT correction show good agreement with the experimental values [3]. And the SCT correction has been applied widely to evaluate the rate constants in the heavy-light-heavy mass combination for the hydrogen abstraction reactions [30–32], such as the reactions F + CF_3CH_2F, F + CF_3CH_2Cl, Cl + CH_2Br_2, and Cl + $CHBr_3$. So, it is suitable for the rate constants including the SCT correction for the present study.

Figure 4 shows that it can also be found that the values of k_{2c} are much larger than those of k_{2a}, $k_{2b\text{-}in}$, $k_{2b\text{-}out}$, and k_{2d} by about 1–5, 1–3, 1–4, and 8–26 orders of magnitude in the temperature range 200–600 K. Thus, on the basis of our calculation, the H-displacement channel R2c to yield $Si(CH_3)_3Br$ and H is the major reaction channel in the lower temperature range, which is in accordance with its kinetic superiority. A similar conclusion can be made for the reaction R1 (see Fig. 5).

To further understand the reaction mechanism of the title reaction, the temperature dependence of branching ratios $k_{na}/(k_{na} + k_{nb} + k_{nc} + k_{nd})$, $k_{nb}/(k_{na} + k_{nb} + k_{nc} + k_{nd})$, $k_{nc}/(k_{na} + k_{nb} + k_{nc} + k_{nd})$, and $k_{nd}/(k_{na} + k_{nb} + k_{nc} + k_{nd})$ ($n = 1, 2$) are calculated and exhibited against the reciprocal of temperature in Figs. 6, 7. From Fig. 6, it can be seen that the H-displacement channel from SiH group R2c is to dominate the reaction in the lower temperature region. The value of $k_{2c}/(k_{2a} + k_{2b} + k_{2c} + k_{2d})$ is greater than or equal to 91% in the temperature range 200–450 K. This is consistent with the inferences made from the potential barrier heights of these five reaction channels. For reaction R2a, increasing temperature, the contribution of k_{2a} and k_{2b} to the overall rate constant increases gradually; for instance, the ratios $k_{2a}/(k_{2a} + k_{2b} + k_{2c} + k_{2d})$ and $k_{2b}/(k_{2a} + k_{2b} + k_{2c} + k_{2d})$ are up to 5–78 and 4–13% from 450 to 1,500 K, respectively, i.e., the reaction channels R2a and R2b become more and more competitive with increasing temperature, especially for R2a. Therefore, the H-abstraction channel from SiH_3 group R2a should be considered when the temperature increases, and R1b should be considered with increasing temperature (see Fig. 7).

As a result of the limited experimental knowledge of the kinetics of the title reaction, we hope that our present study may provide useful information for future laboratory investigations. For the convenience of future experimental measurements, the two-parameter and three-parameter fits of the ICVT/SCT rate constants of five reaction channels and the whole reaction in the temperature range from 200

to 1,500 K are performed, and the expressions are given as follows (in unit of cm^3 $molecule^{-1}$ s^{-1}):

$$k_{1a}(T) = 1.19 \times 10^{-17}\, T^{1.70}\exp(855.62/T)$$
$$k_{1b}(T) = 9.97 \times 10^{-19}\, T^{2.47}\exp(951.87/T)$$
$$k_{1c}(T) = 7.79 \times 10^{-13}\, T^{0.60}\exp(489.83/T)$$
$$k_{1d}(T) = 1.27 \times 10^{-17}\, T^{2.20}\exp(-10,887.64/T)$$
$$k_1(T) = 6.30 \times 10^{-15}\, T^{1.36}\exp(704.94/T)$$
$$k_{2a}(T) = 5.54 \times 10^{-13}\, T^{1.48}\exp(-5,537.88/T)$$
$$k_{2b}(T) = 3.88 \times 10^{-18}\, T^{2.45}\exp(-3,663.28/T)$$
$$k_{2c}(T) = 5.64 \times 10^{-17}\, T^{1.88}\exp(-1,914.63/T)$$
$$k_{2d}(T) = 5.13 \times 10^{-18}\, T^{2.30}\exp(-14,568.38/T)$$
$$k_2(T) = 9.41 \times 10^{-26}\, T^{4.89}\exp(-1,033.80/T)$$

4 Conclusion

In this paper, the multi-channel reactions of $SiH(CH_3)_3$ with Cl and Br atoms are theoretically studied. The potential energy surface information is obtained at the MP2/6-31+G(d,p) level, and energies of the stationary points and a few extra points along the minimum energy path are refined at the MC-QCISD level. For the title reaction, ten reaction channels are identified, and H-displacement channel R2c is the major reaction channel in the lower temperature range 200–600 K. The rate constants for five reaction channels are calculated by the improved canonical variational transition state theory (ICVT) incorporating small-curvature tunneling (SCT) correction at the MC-QCISD//MP2 level. The calculated results show that the tunneling effect for reaction channels R2a and R2d plays an important role at the lower temperatures. The overall ICVT/SCT rate constant, k_2, is in good agreement with the available experimental value. The three-parameter rate-temperature formulae for the Br + $SiH(CH_3)_3$ reaction in the temperature range from 200 to 1,500 K are fitted and given as follows (in cm^3 $molecule^{-1}$ s^{-1}):

$$k_1(T) = 6.30 \times 10^{-15}\, T^{1.36}\exp(704.94/T)$$
$$k_2(T) = 9.41 \times 10^{-26}\, T^{4.89}\exp(-1,033.80/T).$$

Acknowledgments The authors thank Professor Donald G. Truhlar for providing POLYRATE 9.1 program. This work is supported by the National Natural Science Foundation of China (20333050, 20303007, and 20973049), the Program for New Century Excellent Talents in University (NCET), the Doctor Foundation by the Ministry of Education, the Foundation for the Department of Education of Heilongjiang Province (1152G010, 11551077), the Key subject of Science and Technology by the Ministry of Education of China, the SF for Graduate Innovate by the Department of Education of Heilongjiang Province (YJSCX2009-055HLJ), the SF for leading experts in academe of Harbin of China (2011RFJGS026).

References

1. Calvert JG, Atkinson R, Kerr JA, Madronich S, Moortgat GK, Wallington TJ, Yarwood G (2000) The mechanisms of atmospheric oxidation of the alkenes. Oxford, New York
2. Calvert JG, Atkinson R, Becker KH, Kamens RH, Seinfeld JH, Wallington TJ, Yarwood G (2002) The mechanisms of atmospheric oxidation of the aromatic hydrocarbons. Oxford, New York
3. Ding LY, Marshall P (1992) J Am Chem Soc 114:5754
4. Bell RL, Truong TN (1994) J Chem Phys 101:10442
5. Truong TN, Duncan WT, Bell RL (1996) Chemical applications of density functional theory. American Chemical Society, Washington, DC, p 85
6. Truhlar DG (1995) In: Heidrich D (ed) The reaction path in chemistry: current approaches and perspectives. Kluwer, Dordrecht, p 229
7. Corchado JC, Espinosa-Garcia J, Hu W-P, Rossi I, Truhlar DG (1995) J Phys Chem 99:687
8. Hu W-P, Truhlar DG (1996) J Am Chem Soc 118:860
9. Fast PL, Truhlar DG (2000) J Phys Chem A 104:6111
10. Corchado JC, Chuang Y–Y, Fast PL, Villa J, Hu W-P, Liu Y-P, Lynch GC, Nguyen KA, Jackels CF, Melissas VS, Lynch BJ, Rossi I, Coitino EL, Ramos AF, Pu J, Albu TV (2002) POLYRATE version 9.1. Department of Chemistry and Supercomputer Institute, University of Minnesota, Minneapolis
11. Truhlar DG, Garrett BC (1980) Acc Chem Res 13:440
12. Truhlar DG, Isaacson AD, Garrett BC (1985) Generalized transition state theory. In: Baer M (ed) The theory of chemical reaction dynamics, vol 4. CRC Press, Boca Raton, p 65
13. Duncan WT, Truong TN (1995) J Chem Phys 103:9642
14. Frisch MJ, Head-Gordon M, Pople JA (1990) Chem Phys Lett 166:275
15. Head-Gordon M, Pople JA, Frisch MJ (1988) Chem Phys Lett 153:503
16. Frisch MJ, Trucks GW, Schlegel HB, Scuseria GE, Robb MA, Cheeseman JR, Montgomery Jr JA, Vreven T, Kudin KN, Burant JC, Millam JM, Iyengar SS, Tomasi J, Barone V, Mennucci B, Cossi M, Scalmani G, Rega N, Petersson GA, Nakatsuji H, Hada M, Ehara M, Toyota K, Fukuda R, Hasegawa J, Ishida M, Nakajima T, Honda Y, Kitao O, Nakai H, Klene M, Li X, Knox JE, Hratchian HP, Cross JB, Adamo C, Jaramillo J, Gomperts R, Stratmann RE, Yazyev O, Austin AJ, Cammi R, Pomelli C, Ochterski JW, Ayala PY, Morokuma K, Voth GA, Salvador P, Dannenberg JJ, Zakrzewski VG, Dapprich S, Daniels AD, Strain MC, Farkas O, Malick DK, Rabuck AD, Raghavachari K, Foresman JB, Ortiz JV, Cui Q, Baboul AG, Clifford S, Cioslowski J, Stefanov BB, Liu G, Liashenko A, Piskorz P, Komaromi I, Martin RL, Fox DJ, Keith T, Al-Laham MA, Peng CY, Nanayakkara A, Challacombe M, Gill PMW, Johnson B, Chen W, Wong MW, Gonzalez C, Pople JA (2003) Gaussian, Inc., Pittsburgh
17. Garrett BC, Truhlar DG, Grev RS, Magnuson AW (1980) J Phys Chem 84:1730
18. Lu DH, Truong TN, Melissas VS, Lynch GC, Liu YP, Grarrett BC, Steckler R, Issacson AD, Rai SN, Hancock GC, Lauderdale JG, Joseph T, Truhlar DG (1992) Comput Phys Commun 71:235
19. Liu Y-P, Lynch GC, Truong TN, Lu D-H, Truhlar DG, Garrett BC (1993) J Am Chem Soc 115:2408
20. Truhlar DG (1991) J Comput Chem 12:266
21. Chuang YY, Truhlar DG (2000) J Chem Phys 112:1221
22. Kuchitsu K (1998) Structure of free polyatomic molecules basic data, vol 1. Springer, Berlin, p 104

23. NIST Chemistry WebBook, NIST Standard Reference Database Number 69, June 2005 Release, Data compiled by Huber KP, Herzberg G
24. Hammond GS (1955) J Am Chem Soc 77:334
25. Chase Jr MW, Davies CA, Downey JR, Fryrip DJ, McDonald RA, Syverud AN (1985) JANAF thermochemical tables, 3rd edn, Ref. Data 14, 1, Suppl 1
26. In NIST Chemistry WebBook, NIST Standard Reference Database Number 69, June 2005 Release, Vibrational frequency (date compiled by T. Shimanouchi)
27. Chase MW (1998) NIST-JANAF themochemical tables, 4th edn. J Phys Chem Ref Data Monograp 9:1–1951
28. Walsh R (1992) In Energetica of Organometallic species; NATO-ASI series C, 367. In: Martinho Simões JA (ed) Chapter 11, Kluwer, Dordrecht
29. Pacey PD (1981) J Chem Educ 58:612
30. Wang L, Zhao Y, Zhang J, Dai YN, Zhang JL (2011) Theor Chem Acc 128:183
31. Xiao JF, Li ZS, Ding YH, Huang XR, Sun CC (2002) J Mol Struct 582:53
32. Xiao JF, Li ZS, Liu JY, Li S, Sun CC (2003) J Phys Chem A 107:267